JGSP **48** (2018) 1–21

JOURNAL OF
Geometry and Symmetry in Physics
ISSN 1312-5192

UNSTEADY ROTO-TRANSLATIONAL VISCOUS FLOW: ANALYTICAL SOLUTION TO NAVIER-STOKES EQUATIONS IN CYLINDRICAL GEOMETRY

ALESSIO BOCCI, GIOVANNI MINGARI SCARPELLO AND DANIELE RITELLI

Communicated by Ivaïlo M. Mladenov

Abstract. We study the unsteady viscous flow of an incompressible, isothermal (Newtonian) fluid whose motion is induced by the sudden swirling of a cylindrical wall and is also starting with an axial velocity component. Basic physical assumptions are that the pressure axial gradient keeps its hydrostatic value and the radial velocity is zero. In such a way the Navier-Stokes PDEs become uncoupled and can be solved separately. Accordingly, we provide analytic solutions to the unsteady speed components, i.e., the axial $v_z(r,t)$ and the circumferential $v_\theta(r,t)$, by means of expansions of Fourier-Bessel type under time damping. We also find: the surfaces of dynamical equilibrium, the wall shear stress during time and the Stokes streamlines.

MSC: 35Q30, 33C10
Keywords: Bessel functions, Navier-Stokes equations, unsteady flow

Contents

doi: 10.7546/jgsp-48-2018-1-21

1. Introduction

1.1. On the Navier-Stokes Equations

The Navier-Stokes system constitutes the balance between the rate of change of momentum of a fluid element and the forces on it, as the Newton's second law does for a particle. Newton himself started (*Principia*, 1687) the dynamics of a viscous fluid in a rather intuitive form: a definitive theory would come much later. The second law was applied by Euler in his seminal memoir [7] of 1757, where he provided a system of PDE ruling a *frictionless* fluid motion, compressible or not, under an arbitrary set of external forces, while his antecessors had worked on incompressible fluids only, with one (as done by Daniel Bernoulli and Johann Bernoulli) or two (as D'Alembert) degrees of freedom.

At the beginning of the 19th century, elasticity was an important asset to engineers looking for a sound theory of the beam bending. In 1827, Navier (1785-1836), the founder of modern structural analysis, extended, see [16], his theory to hydrodynamics: this led him to insert in Euler's equations a new $\mu-$force, (being μ the dynamical viscosity of the fluid, namely a measure of its internal friction) revealed by the non-uniformity of the motion itself. Stokes (1819-1903), [19], reviewing the work of Navier and others, presented in 1849 a short rational approach to the equations of *viscous fluids* arriving to the Navier-Stokes equations, as we now know them: they are applicable also to non-Newtonian fluids (i.e., whose stress is not linearly related to the strain rate), and to both laminar and turbulent flows of liquid/gas.

The main difficulty with the Navier-Stokes equations is due to their nonlinearity arising from the convective acceleration terms, see (1). For most flow problems, fluid particles really do have acceleration as they move from one location to another in the flow field: so that the convective acceleration terms usually cannot be neglected. However, there are a few special cases, as in our paper, where the convective acceleration vanishes, for instance due to the flow system symmetry or to other causes. In such cases exact solutions become possible for an unsteady problem too.

We say "exact solution", as done for instance in [11], to denoting an explicit formula in terms either of elementary or special functions, in contrast to "approximate solution", which approximates a solution either in a numerical sense or in its asymptotic limit, e.g. with a vanishingly small viscosity, and so on. Anyway, no one of them can capture the long time behavior of phenomena. From the early 20^{th} century, asymptotic methods extended the range of tractable problems and numerical methods have been more and more reliable. Nevertheless the exact solutions remain a valuable resource: they allow cross-checks of some numerical approaches and immediately convey more physical insight than all the numerical tables one could compute, specially for systems ruled by parameters for whom a complete numerical tabulation would be neither practical nor clear.

The functions appearing in our solutions are infinite series and Bessel functions of integer order and by their analytic structure we are allowed to infer the main flow behaviors without long computations.

1.2. Outline of Some Contemporary Literature

There are not many unsteady analytical Navier-Stokes solutions concerning a Newtonian, incompressible fluid. We would then exclude some sound treatments like those of Ayub *et al* [10] where our same aim is pursued but for fluids (those of magnetohydrodynamics) by a far different nature. In [5] is analyzed a planar problem with a viscous fluid hold within an annulus where both inner and outer cylinder walls may be rotating, while [15] studies a purely axial flow induced by the sudden axial motion of a cylinder in a fluid initially at rest. The Batchelor's treatise [2] founds his treatments on the Stokes standard solution with the error function, trying to put back each unsteady one dimensional problem to that one. Drazin and Riley in [6] cover the unsteady state. Chapter 4 describes some unsteady flows bounded by plane boundaries: the angled flat plate motion is solved through the confluent Kummer hypergeometric function. Chapter 5 is devoted to the unsteady axisymmetric flow in pipes. The pulsed flow, namely with a periodic pressure gradient (also called Womersley's flow) is also discussed. The article of Knyazev [11] founds on the so called Karmán family of the Navier-Stokes exact solutions. Some non-self-similar solutions are considered to solve the problem of an unsteady incompressible flow between two rotating disks, one of which moves along the common rotation axis. Detailed plots represent the solutions computed in terms of elementary functions, though the expressions are quite intricate. In [13] first of all Langlois and Deville analyze the motion of a viscous fluid produced by a flat plate in a direction parallel to it. It may be either steady from a starting instant on (first Stokes problem: flow in a semi-infinite space), or periodic in time (second Stokes problem). Since the plate oscillates with frequency $\cos(\omega t)$, a reasonable guess solution can be $u(y,t) = f(y)\exp(\mathrm{i}\omega t)$. It is also treated the transient of the channel flow with a pulsatile pressure gradient or a Poiseuille flow with the pipe wall forced by a torsional oscillation. An interesting problem is that of a spherical R-bubble of inviscid gas included in an unlimited liquid: assuming the gas pressure variable with time, the radius of the bubble will also change with time. Such a pulsating bubble will generate a velocity field within the liquid which in turn produces a stress field. At the end one is led to a second order non-linear differential equation, for which Langlois refers to his original articles. In the recent book of Brenn [4] the hydrodynamic problem is faced not directly through the velocity components but via the Stokes stream function PDE. Another case: flow fields along infinite structures without any geometrical elements with length scales, for instance along flat plates, without an imprinted flow time scale. In every case, the form assumed for the velocity profile caused the nonlinear inertia terms in the Navier-Stokes equation either to vanish completely or to produce only a centrifugal force, easily balanced by a pressure gradient.

In some cases the unsteady problem will lead to some nonlinear ODE as in Shapiro's paper [18] about an unsteady axisymmetric incompressible case with a uniform injection or suction from a porous boundary (plate), arriving at a third order nonlinear ODE which can be transformed into a Riccati tractable equation.

The exactly-solved unsteady problems are then concerning some few and simple geometries, but different physical conditions. The mathematical tools are: similarity variable transformation, variable separation, eigenfunctions expansion; several special functions are then involved. It is less seen the employ of integral transforms of Fourier or Laplace, probably due to difficulties with the Bromwich contour integration.

1.3. Aim of the Work

Let us consider a cylindrical vessel of internal radius R with a vertical upward axis, say z, that at time $t = 0$ is put in rotation with angular velocity $\boldsymbol{\omega} = \Omega\boldsymbol{k}$, $\Omega \in \mathbb{R}$ being the modulus of the angular velocity which is kept constant during time. The vessel holds an incompressible liquid initially at rest: we will study its unsteady viscous motions in both directions, that is *axial* and *circumferential* (or *tangential*). The liquid is under the steady loads of centrifugal and gravitational nature and, in addition, to a vertical outside pulse, at the start up only, which is responsible of the initial axial upward velocity $v_z^0 > 0$. The velocity field $\mathbf{v} = (v_r, v_\theta, v_z)$ for the laminar incompressible viscous flow is ruled by the Navier-Stokes equations in cylindrical coordinates $(r,\ \theta,\ z)$

$$\rho\left[\frac{\partial v_r}{\partial t} + v_r\frac{\partial v_r}{\partial r} + \frac{v_\theta}{r}\frac{\partial v_r}{\partial \theta} - \frac{v_\theta^2}{r} + v_z\frac{\partial v_r}{\partial z}\right]$$
$$= -\frac{\partial P}{\partial r} + \mu\left[\frac{\partial}{\partial r}\left(\frac{1}{r}\frac{\partial(r v_r)}{\partial r}\right) + \frac{1}{r^2}\frac{\partial^2 v_r}{\partial \theta^2} - \frac{2}{r^2}\frac{\partial v_\theta}{\partial \theta} + \frac{\partial^2 v_r}{\partial z^2}\right] + \rho g_r \quad (1a)$$

$$\rho\left[\frac{\partial v_\theta}{\partial t} + v_r\frac{\partial v_\theta}{\partial r} + \frac{v_\theta}{r}\frac{\partial v_\theta}{\partial \theta} + \frac{v_r v_\theta}{r} + v_z\frac{\partial v_\theta}{\partial z}\right]$$
$$= -\frac{1}{r}\frac{\partial P}{\partial \theta} + \mu\left[\frac{\partial}{\partial r}\left(\frac{1}{r}\frac{\partial(r v_\theta)}{\partial r}\right) + \frac{1}{r^2}\frac{\partial^2 v_\theta}{\partial \theta^2} + \frac{2}{r^2}\frac{\partial v_r}{\partial \theta} + \frac{\partial^2 v_\theta}{\partial z^2}\right] + \rho g_\theta \quad (1b)$$

$$\rho\left[\frac{\partial v_z}{\partial t} + v_r\frac{\partial v_z}{\partial r} + \frac{v_\theta}{r}\frac{\partial v_z}{\partial \theta} + v_z\frac{\partial v_z}{\partial z}\right]$$
$$= -\frac{\partial P}{\partial z} + \mu\left[\frac{1}{r}\frac{\partial}{\partial r}\left(r\frac{\partial v_z}{\partial r}\right) + \frac{1}{r^2}\frac{\partial^2 v_z}{\partial \theta^2} + \frac{\partial^2 v_z}{\partial z^2}\right] + \rho g_z \quad (1c)$$

hereinafter called radial (1a), circumferential (1b), axial (1c), ones, respectively.

Setting the non-vertical components of gravity to zero and the vertical one to $-g$, we assume that the velocity radial component vanishes, for any $r,\ \theta,\ z,\ t$, thus $\mathbf{v} = (0,\ v_\theta(r,t),\ v_z(r,t))$. As a consequence the circumferential and axial equations of the Navier-Stokes system become uncoupled and can be treated separately, as explained below.

- Equation (1c) in the unknown v_z. We assume the axial pressure gradient does not differ from its hydrostatic asset, namely: $\partial P/\partial z = -\rho g$. In such a way we will find separately $v_z(r,t)$ as independent on the height z. Such a velocity component must meet the upwards initial condition $v_z(r,0) = v_z^0 > 0$ and in addition the *no-slip* one around the circular boundary: $v_z(R,t) = 0$, for any $t > 0$. Finally, when the transient is off, v_z has to be extinguished, not being any physical reason for any vertical motion going on during time.

- Equation (1b). Assuming v_θ does not depend on z, we will not do any further special assumption.

- Equation (1a) becomes

$$\rho\frac{v_\theta^2}{r} = \frac{\partial P}{\partial r} \quad (2)$$

then, after v_θ has been computed, we will integrate the pressure scalar field $P(r, z, t)$ whose axial gradient had been assumed known. Equation (2) constitutes the nonlinearity of the Navier-Stokes system studied here. Furthermore the computation of v_θ implies that we can evaluate the unsteady equilibrium surfaces of liquid and the wall shear stress as well.

2. The Axial Sub-Problem

Let the z-velocity component depend on r and t only: $v_z = v_z(r, t)$ and the z-transient flow does not affect the pressure axial gradient along such a direction

$$\frac{\partial P}{\partial z} = -\rho g.$$

This does not imply that the unsteady overpressures are physically much less than the relevant static ones but only that axial pressure gradient is conditioned only by weights and heights, so that it changes little due to the small change in height. With these assumptions, the axial Navier-Stokes (1c) becomes linear

$$\frac{\partial v_z}{\partial t} = \frac{\nu}{r}\frac{\partial}{\partial r}\left(r\frac{\partial v_z}{\partial r}\right). \tag{3}$$

Equation (3) has to be solved imposing conditions

$$v_z(0, t) \in \mathbb{R}, \qquad v_z(R, t) = 0, \qquad v_z(r, 0) = v_z^0. \tag{4}$$

Where the first of (4) ensures finite velocity along the axis, the second is the no-slip condition, since the liquid velocities appearing in all previous formulæ are all absolute: as adherent to the wall, the liquid shall be as the wall itself at rest, so that the second relation in (4) must hold. Finally the third of (4) is the initial condition and v_z^0 is the value, which we assume positive, of the initial upwards velocity common to each r.

2.1. Axial Sub-Problem Outline

We solve (3) by separation of variables: $v_z(r, t) = F(r)T(t)$. Marking by a dot the time derivative and by $'$ the spatial derivative, we obtain

$$\dot{T} = -\eta^2 T, \qquad F'' + \frac{F'}{r} + \frac{\eta^2}{\nu}F = 0 \tag{5}$$

where η is an unknown separation constant. The second equation in (5) is a Bessel equation whose general solution is

$$F(r) = CJ_0\left(\frac{\eta}{\sqrt{\nu}}r\right) + DY_0\left(\frac{\eta}{\sqrt{\nu}}r\right), \qquad C,\, D \in \mathbb{R} \tag{6}$$

where J_0 is the Bessel function of first kind and zero order and Y_0 that of second kind and zero order. By (4), we detect the integration constants of (6) and then solve (3). From the finiteness condition, the first of (4), it shall be $D = 0$, since Y_0 is unbounded in a neighbourhood of the origin. Imposing the non-slip condition, that is the second of (4), we obtain a sequence of values of η connected to the zeros of of J_0, i.e., $\eta_n = \sqrt{\nu}\beta_n/R$ where $(\beta_n)_{n\in\mathbb{N}}$ is the infinite sequence of the zeros of J_0. Thus we obtain, writing $\sigma_n = \beta_n/R$, the infinite sequence of eigenfunctions

$$v_{z_n}(r,t) = C_n J_0(\sigma_n r)\mathrm{e}^{-\nu\sigma_n^2 t}.$$

In such a way the initial axial value v_z^0 can be represented as a series of eigenfunctions

$$v_z^0 = \sum_{n=1}^{+\infty} C_n J_0(\sigma_n r)$$

and each of them is connected to J_0's roots. Then, integrating between $r = 0$ and $r = 1$, recalling the orthogonality properties of Bessel functions as expressed by the Lommel integrals, we get

$$C_n = v_z^0 \frac{\displaystyle\int_0^1 r\, J_0(\sigma_n r)\,\mathrm{d}r}{\displaystyle\int_0^1 r\, J_0^2(\sigma_n r)\,\mathrm{d}r} = v_z^0 \frac{\dfrac{1}{\sigma_n} J_1(\sigma_n)}{\dfrac{1}{2} J_1^2(\sigma_n)} = \frac{2v_z^0}{\sigma_n\, J_1(\sigma_n)}.$$

The axial unsteady flow is then ruled by

$$v_z(r,t) = 2v_z^0 \sum_{n=1}^{+\infty} \frac{J_0(\sigma_n r)}{\sigma_n J_1(\sigma_n)} \mathrm{e}^{-\nu\sigma_n^2 t}. \tag{7}$$

A large collection of 19^{th}-century literature about the roots of Bessel functions is available: we will refer to McMahon formula [14], quoted also in [1, p 371]. Specialized to our case, after some manipulation we arrive at

$$\beta_n = \pi(n-0.25) + \frac{1}{8\pi(n-0.25)} - \frac{31}{384\pi^3(n-0.25)^3} + \frac{3779}{15360\pi^5(n-0.25)^5} - \frac{6277237}{3440640\pi^7(n-0.25)^7} + \cdots$$

We then compute the unsteady axial velocity: it can be used to investigate the flow changes produced by starting the rotation of the circular cylinder and the subsequent approach to a steady state. Fig. 1 obtained using Mathematica® shows the imposed uniform initial value v_z^0, the fixed points of vanishing v_z at the round boundary, and all the declining profiles, whose maximum is gradually reduced with time, until its complete extinction.

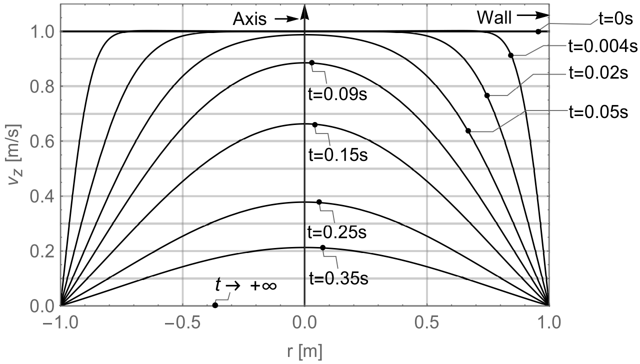

Figure 1. Unsteady axial velocity $v_z(r,t)$ with $v_z^0 = 1$, $R = 1$, $\nu = 1$.

Remark 2.1 *Observe that for any $t > 0$ the volume flux across any section of the unsteady axial flow field is*

$$Q(t) = 2\pi \int_0^R v_z(r,t)\, r \,\mathrm{d}r$$

so that the total volume will be

$$\int_0^{+\infty} Q(t)\,\mathrm{d}t.$$

From (7) *such volume can be computed by means of Bessel functions theorems.*

3. The Circumferential Sub-Problem

For this problem the treatment will be longer due to the constraint between the circumferential velocity v_θ and the radial pressure gradient. In addition, the PDE ruling the velocity is less simple. The relevant assumptions are:

- At a fixed r-value, the circumferential velocity component does not change with the angle θ and the height z: $v_\theta = v_\theta(r,t), \quad$ for any $\theta,\ z$.

- Pressure P depends on time t because we are dealing with an unsteady flow; on r due to centrifugal force; and, finally, on z due to gravity. In addition there is no pressure gradient along the direction θ, so that $P = P(r,z,t)$, for any θ.

- The radial component of velocity is assumed to be identically zero, i.e. $v_r = 0$ for any $r,\ \theta,\ z,\ t$.

In circumferential (1b), and radial (1a) Navier-Stokes equations, setting to zero the pressure circumferential gradient, the radial velocity, the derivatives of v_θ with respect to θ and z, we get

$$\rho\frac{v_\theta^2}{r} = \frac{\partial P}{\partial r}, \qquad \rho\frac{\partial v_\theta}{\partial t} = \mu\frac{\partial}{\partial r}\left(\frac{1}{r}\frac{\partial(rv_\theta)}{\partial r}\right), \qquad \frac{\partial P}{\partial z} = -\rho g \tag{8}$$

Remark 3.1 *Notice that the first of the equations above shows that the radial variation of pressure simply supplies the force necessary to keep the fluid elements moving in a circular path within the vessel.*

Remark 3.2 *In this situation the continuity equation*

$$\frac{\partial\rho}{\partial t} + \frac{1}{r}\frac{\partial}{\partial r}(\rho r v_r) + \frac{1}{r}\frac{\partial}{\partial\theta}(\rho v_\theta) + \frac{\partial}{\partial z}(\rho v_z) = 0$$

holds for any t and for each point inside the fluid.

3.1. Circumferential Sub-Problem Outline

Ought to problem's linearity following [20], we represent $v_\theta(r,t)$ as

$$v_\theta(r,t) = v_\theta^\infty(r) - \hat{v}(r,t) \tag{9}$$

namely by adding to the steady state circumferential velocity distribution an unknown component $\hat{v}(r,t)$ depending on space and time. The steady state solution $v_\theta^\infty(r)$ is found as follows: putting $\nu = \mu/\rho$ (kinematic viscosity), recalling that $\partial_t v_\theta^\infty = 0$, by the second of (8) we have

$$\frac{\partial}{\partial r}\left(\frac{1}{r}\frac{\partial}{\partial r}\left(r\, v_\theta^\infty(r)\right)\right) = 0.$$

Integrating, we obtain, being K_1 and K_2 constants of integration

$$v_\theta^\infty(r) = \frac{K_2}{r} + \frac{K_1}{2}r.$$

We have to impose $K_2 = 0$ in order to deal with finite solution. Furthermore, due to the boundary condition it shall be $v_\theta^\infty(R) = \Omega R$, therefore $K_1 = 2\Omega$, so that: $v_\theta^\infty(r) = \Omega r$. Inserting in (9) we obtain

$$v_\theta(r,t) = \Omega r - \hat{v}(r,t). \tag{10}$$

We then have the equation of the circumferential transient velocity $\hat{v}(r,t)$

$$\frac{\partial\hat{v}(r,t)}{\partial t} = \nu\left(\frac{\partial^2\hat{v}(r,t)}{\partial r^2} + \frac{1}{r}\frac{\partial\hat{v}(r,t)}{\partial r} - \frac{\hat{v}(r,t)}{r^2}\right) \tag{11}$$

which is linear and to be solved imposing the following conditions

$$\hat{v}(0,t) \in \mathbb{R}, \qquad \hat{v}(R,t) = 0, \qquad \hat{v}(r,0) = \Omega r. \tag{12}$$

The first condition in (12) ensures that along the z-axis the velocity shall always be finite. The second equation (12) ensures adhesion to wall, usually referred as no-slip condition: it implies a velocity which shall for any $t > 0$ be stuck on the value ΩR of the cylinder circumferential velocity. In order to meet this, the unsteady contribution at $r = R$ shall be zero at any time. Finally the third of (12) is the functional type initial condition. To similar mathematical model, but as *external* motion, arrive other authors as [12] and [6].

3.2. Integration of Equation (11)

We now perform the integration of (11). We use the standard change of variable $r = \mathrm{e}^x$, $\hat{v}(r,t) = u(x,t)$. Thus we can express the partial derivatives of u with respect to x as

$$\frac{\partial \hat{v}}{\partial r} = \frac{\partial u}{\partial x}\frac{\partial x}{\partial r} = \frac{1}{r}\frac{\partial u}{\partial x}$$

$$\frac{\partial^2 \hat{v}}{\partial r^2} = \frac{\partial}{\partial r}\left(\frac{1}{r}\frac{\partial u}{\partial x}\right) = -\frac{1}{r^2}\frac{\partial u}{\partial x} + \frac{1}{r}\frac{\partial^2 u}{\partial x^2}\frac{\partial x}{\partial r} = -\frac{1}{r^2}\frac{\partial u}{\partial x} + \frac{1}{r^2}\frac{\partial^2 u}{\partial x^2}.$$

So that

$$\frac{\partial u(x,t)}{\partial t} = \frac{\nu}{\mathrm{e}^{2x}}\left[\frac{\partial^2 u(x,t)}{\partial x^2} - u(x,t)\right].$$

Let us look for a solution, again by separation $u(x,t) = X(x)T(t)$ obtaining

$$\dot{T} = -\lambda^2 T, \qquad X'' + \frac{\left(\lambda^2 \mathrm{e}^{2x} - \nu\right)}{\nu} X = 0 \tag{13}$$

with λ being the separation constant set yet to be found. First equation in (13) leads to $T(t) = \mathrm{e}^{-\lambda^2 t}$, while the solution of the second (spatial) equation in (13) is represented in terms of Bessel functions, see [17, p 246]

$$X(x) = C J_1\left(\frac{\lambda}{\sqrt{\nu}}\mathrm{e}^x\right) + D Y_1\left(\frac{\lambda}{\sqrt{\nu}}\mathrm{e}^x\right). \tag{14}$$

To detect the integration constants C, D in (14) we impose the relevant conditions (12), proceeding as in Section 2. First we impose the finiteness of the solution, see first condition in (12), therefore we must take $D = 0$ in (14). So that here we connect to the zeros of J_1 obtaining the infinte sequence of eigenfunctions

$$\hat{v}(r,t) = C_n J_1\left(b_n r\right)\mathrm{e}^{-\nu b_n^2 t} \tag{15}$$

where the eigenvalues λ_n associated to the separation constant are determined as: $\lambda_n = \sqrt{\nu}\alpha_n/R$ where $(\alpha_n)_{n\in\mathbb{N}}$ represents the sequence of zeros of the first kind and first order Bessel function J_1, see [8], and where, for simplicity, we introduced $b_n = \alpha_n/R$. Lastly we impose the initial finiteness condition obtained from the third of (12). Let us express the continuity of the junction between the velocity distributions in the sense that at the initial time the transient component must equate the steady component due to the fact that the overall velocity v_θ shall for any r be zero at the start-up $v_\theta(r,0) = 0$ implies $\hat{v}(r,0) = v_\theta^\infty(r)$, this is the initial condition for $r \in [0,R]$. The problem will be solved by expanding in a series of eigenfunctions the function Ωr: the relevant coefficients C_n have to be computed founding on the fact that the family of the eigenfunctions forms an orthonormal complete system

$$\sum_{n=1}^{+\infty} C_n J_1\left(b_n r\right) = \Omega r.$$

The coefficients C_n, can be found by multiplying both sides of the above expansion by $r\, J_1(b_m r)$ having fixed a particular integer m and integrating for r from 0 to 1, so that

$$\int_0^1 \sum_{n=1}^{+\infty} C_n\, r J_1(b_n r) J_1(b_m r)\,\mathrm{d}r = \Omega \int_0^1 r^2\, J_1(b_m)\,\mathrm{d}r.$$

Due to Bessel functions orthogonality and Lommel integrals, only the integral with $n = m$ does not vanish, that is

$$C_m = \frac{\Omega \displaystyle\int_0^1 r^2\, J_1\left(b_m r\right)\, \mathrm{d}r}{\displaystyle\int_0^1 r\, J_1^2\left(b_m r\right)\, \mathrm{d}r}.$$

For the integral at numerator see entries 6.561.5 and 6.521.1 of [9]. Then we found the eigenvalues discrete spectrum of C_n for any $n \in \mathbb{N}$

$$C_n = \Omega \frac{\left(b_n\right)^{-1} J_2\left(b_n\right)}{\frac{1}{2} J_2^2\left(b_n\right)} = \frac{2\Omega}{b_n\, J_2\left(b_n\right)}$$

with J_2 being the first kind, order two Bessel function. So

$$\hat{v}(r,t) = 2\Omega \sum_{n=1}^{+\infty} \frac{J_1(b_n r)}{b_n J_2(b_n)} \mathrm{e}^{-\nu b_n^2 t}. \tag{16}$$

Therefore the overall circumferential velocity is given by

$$v_\theta(r,t) = \Omega r - 2\Omega \sum_{n=1}^{+\infty} \frac{J_1(b_n r)}{b_n J_2(b_n)} \mathrm{e}^{-\nu b_n^2 t}. \tag{17}$$

Again, as previously for roots β_n of J_0, in order to compute all roots α_n of J_1 function, we will adapt the McMahon formula

$$\begin{aligned}\alpha_n =&\pi(0.25+n) - \frac{3}{8\pi(0.25+n)} + \frac{3}{128\pi^3(0.25+n)^3}\\ &- \frac{1179}{5120\pi^5(0.25+n)^5} + \frac{1951209}{1146880\pi^7(0.25+n)^7} - \cdots\end{aligned}$$

being $n = 1, \ldots, +\infty$ the marker of the n-th zero of J_1.

3.3. A Profile Analysis of v_θ

For all next computations, we took (SI units): $\Omega = 1,\ R = 1,\ \nu = 1$. The transient component $\hat{v}(r,t)$ is given by (16).

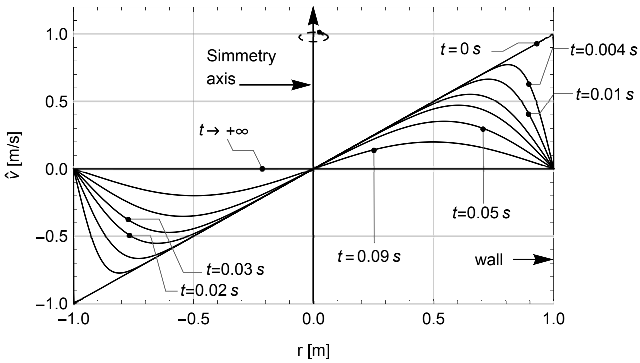

Figure 2. Circumferential velocity unsteady response $\hat{v}(r,t)$ profiles.

At the start-up, being $\hat{v}(r,0) = v_\theta(r)$, the transient begins with a linear behaviour. Notice that we used thousands terms in the series (16) for earning a correct representation of the linear profile in terms of a Fourier-Bessel expansion. Declining the transient with time, the plot will twist in the curves shown in Fig. 2, up to its extinction. Furthermore notice that, by setting to zero, for a fixed time $\bar{t}$, the derivative with respect to r of (16), we get an expression like

$$\sum_{n=1}^{+\infty} \frac{\mathrm{e}^{-\nu b_n^2 \bar{t}}}{J_2(b_n)} \cdot \frac{\mathrm{d}J_1}{\mathrm{d}r}(b_n\bar{r}) = 0$$

$\bar{r}$ being the $r > 0$ value maximizing $\hat{v}(r)$. All the performed simulations showed that, for increasing time, the $\bar{r}$ sequence decreases. This is due to the exponential decay-law which rules the $\mathrm{d}J_1/\mathrm{d}r$ to vanish for $r \to 0^+$. When time increases, the exponential factor loses its weight and then the maximum of $\hat{v}$ does not change its position any more, see (Fig. 2). The overall velocity v_θ profile is then shown by (Fig. 3).

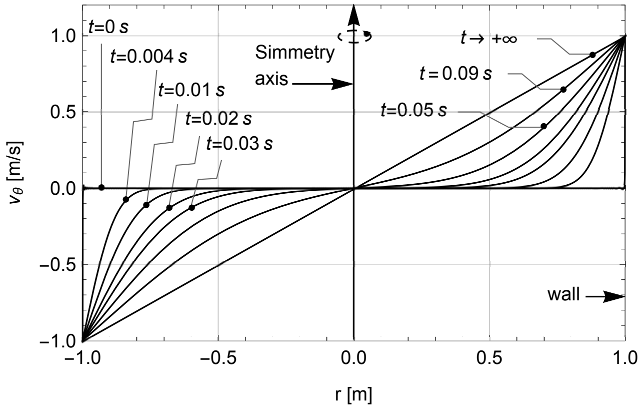

Figure 3. Circumferential overall velocity profiles, $v_\theta(r,t)$.

3.4. The Pressure Field

Integrating the first of (8) we obtain

$$P(r,z,t) = \rho \int_0^r \frac{v_\theta^2(\psi,t)}{\psi} \mathrm{d}\psi + f(z,t) + \beta. \tag{18}$$

The pressure axial gradient $f(z,t)$ is given by $-\rho g$, and, in order to compute the integration constant β it will be enough to impose the condition: $P(0,0,t) = P_0$ being P_0 an arbitrary value. Then $\beta = P_0$. In such a way, the pressure field expressed by (18) becomes

$$P(r,z,t) = \rho \int_0^r \frac{v_\theta^2(\psi,t)}{\psi} \mathrm{d}\psi - \rho g z + P_0. \tag{19}$$

Inserting in (19) the v_θ law, we obtain

$$P(r,z,t) = P_0 - \rho g z + \frac{\rho r^2 \Omega^2}{2} + \rho \int_0^r \frac{\hat{v}^2(\psi,t)}{\psi} \mathrm{d}\psi - 2\rho\Omega \int_0^r \hat{v}(\psi,t) \mathrm{d}\psi. \tag{20}$$

So, in the full expression (20) of the overall pressure, to the hydrostatic component three further dynamic components are added and two of them are due to $\hat{v}$ so that they will decay with time.

Remark 3.3 *After the unsteady state is over, the steady velocity is* $v_\theta^\infty(r) = \Omega r$ *and, then, inserting in* (19) *we have*

$$P(r, z, \infty) = \frac{\rho\Omega^2}{2} r^2 - \rho g z + P_0$$

namely, the well-known steady pressure distribution of centrifugal-gravitational nature.

3.5. The Liquid Free Surface $z(r, t)$

In (20) we solve with respect to z the equation $P(r, z, t) = P_0$, being P_0 a given real number: it means that we are looking for the space locus of the liquid points for which the internal pressure equates the atmospheric one, i.e. how the liquid free surface is shaped in space and time. We begin introducing a first simplification, taking into account the effect of the simultaneous transient and stationary terms of v_θ, which leads us to approximate $z(r, t)$ obtained from (20) as

$$z(r, t) = \frac{1}{g}\left[\Omega^2 \frac{r^2}{2} - 2\Omega \int_0^r \hat{v}(\psi, t) \mathrm{d}\psi\right]. \tag{21}$$

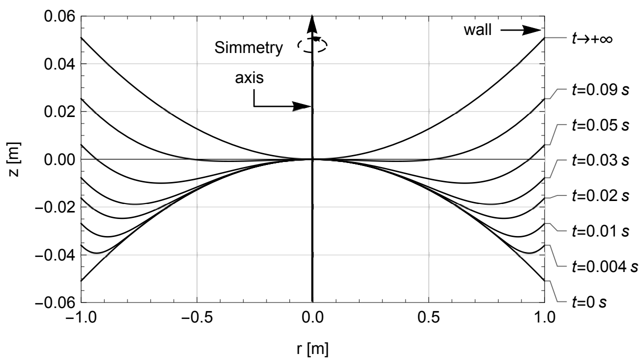

Figure 4. The liquid free surface $z(r, t)$: transient response profiles. First approximation, $\frac{\hat{v}^2(r,t)}{r} = \mathrm{o}(1)$.

We discarded the penultimate term in the left hand side of formula (20) as subjected to a more intense drop during time. (Fig. 4) shows that, immediately after the start-up, the intersection of the liquid round surface with any plane holding the axis of rotation, provides an array of initially concave lines. In an instant between $0\ s$ and $0.004\ s$ (that can be calculated numerically), there is a change of curvature. Next, the curves become convex till when, extinguished almost the transient ($t >$

$0.09\ s$), the free surface takes the known shape of round paraboloid. The surface description does not seem acceptable at the beginning, when the contributions to the overall solution, brought by the integral quadratic which we neglected, are not yet negligible. Recalling that for $t = 0$ we have $v_\theta = 0$ and then from (19) we get $z(r,t) = 0$. Through numerical computation in (20), the overall solution of the free round surfaces is shown in (Fig. 5) which represents some level curves of $z(r,t)$. We observe that profile of such contour curves is initially flat for any r, as

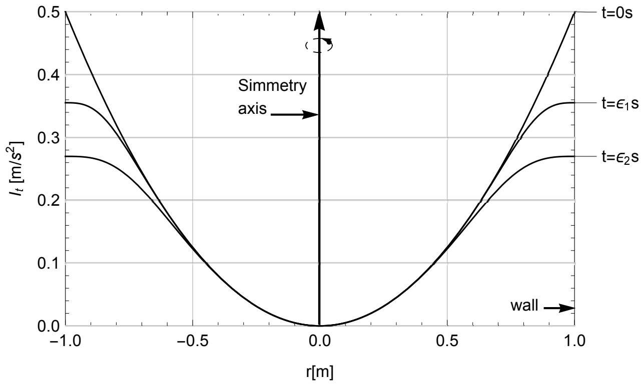

Figure 5. The unsteady free surfaces profiles $z(r,t)$: full evaluation.

expected. The height $z(r,t)$ is given by

$$z(r,t) = \frac{1}{g}\left[\Omega^2\frac{r^2}{2} + \int_0^r \frac{\hat{v}^2(\psi,t)}{\psi}\mathrm{d}\psi - 2\Omega\int_0^r \hat{v}(\psi,t)\mathrm{d}\psi\right].$$

By the initial condition $\hat{v}(r,0) = \Omega r$, we take that

$$\frac{\hat{v}^2(r,t)}{r} = \Omega\frac{\hat{v}^2(r,t)}{\hat{v}(r,0)}$$

and therefore, since we need to study the t-dependence of the following integral, we introduce

$$I(t,r) = \int_0^r \frac{\hat{v}^2(\psi,t)}{\psi}\,\mathrm{d}\psi = \Omega\int_0^r \frac{\hat{v}^2(\psi,t)}{\hat{v}(\psi,0)}\,\mathrm{d}r. \tag{22}$$

We now establish a map of the time evolution of the integral $I(t)$ which is plotted by a different r-curve for each t. At start-up by (22) we get

$$I(0,r) = \Omega\int_0^r \hat{v}(\psi,t)\mathrm{d}\psi = \Omega^2\int_0^r \psi\,\mathrm{d}\psi = \frac{\Omega^2}{2}r^2.$$

At time $t_\varepsilon = 0 + \varepsilon$ with ε small, we will get

$$I(\varepsilon, r) = \Omega \int_0^r \frac{\hat{v}^2(\psi, \varepsilon)}{\hat{v}(\psi, 0)} \, \mathrm{d}r < I(0) = \frac{\Omega^2}{2} r^2$$

provided that $\hat{v}(r, \varepsilon) < \hat{v}(r, 0)$ as shown by Fig. 2. Therefore for each t_ε the curves plotting the integral $I(t, r)$ will lay below the parabola graph of the integral $I(0, r)$. For $t \to +\infty$ clearly we have $I(\infty, r) = 0$.

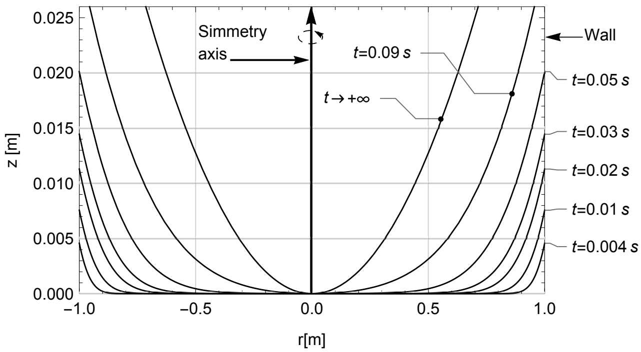

Figure 6. Time evolution of integrals $I(t)$, for some t, with $\varepsilon_2 > \varepsilon_1$.

4. Fluid Motion Representations

In this section we are going to compute some quantitative elements which better define and clarify the motion characters as streamlines and shear stress.

4.1. Streamlines

We provide as $\mathrm{d}r$, $r\mathrm{d}\theta$, $\mathrm{d}z$ the elements of the arc differential of the streamline using cylindrical coordinates. Thus we have $\mathrm{d}\mathbf{s} = \mathrm{d}r \, \mathbf{e}_r + r \, \mathrm{d}\theta \, \mathbf{e}_\theta + \mathrm{d}z \, \mathbf{k}$. So for a rotationally symmetric flow, we have by the streamlines definition $\mathbf{v} \wedge \mathrm{d}\mathbf{s} = \mathbf{0}$. In our specific case, given any instant t_0 (after it has to be considered as a variable parameter $\mathbb{R}^+$), we will get

$$v_\theta(r, t_0)\mathrm{d}z = r v_z \mathrm{d}\theta, \qquad v_z \mathrm{d}r = 0, \qquad v_\theta(r, t_0)\mathrm{d}r = 0. \tag{23}$$

By the second and the third equation in (23) we soon infer it shall be $r = r_0 = \mathrm{constant}$ so that, inserting in the first of (23) and by integration with respect to z, we get a double infinity of streamlines which are helices

$$\theta(r_0, t_0; z) = \frac{v_\theta(r_0, t_0)}{r_0 v_z(r_0, t_0)} z + \kappa_0 \tag{24}$$

being $z \in [0, H]$, $\theta \in [0, 2\pi]$, $\kappa_0 = \theta(r_0, t_0, 0)$.

4.2. Shear Stress $\tau_{r,\theta}$ at the Wall During Time

Any real fluid (liquid or gas) moving along a solid boundary, will undergo a shear stress exerted by the wall. The no-slip condition dictates that the velocity of the fluid relative to the boundary is zero. But at some distance from the boundary, the flow speed must equate that of the unperturbed stream. The region between these two points is aptly named *the boundary layer*. For all Newtonian fluids in laminar flow the shear stress is proportional to the strain rate in the fluid, the viscosity being the constant of proportionality. Knowing the velocity field, we may derive the shear stress in the viscous fluid due to the spinning wall with the no-slip condition on its surface. Let $\tau_{r,\theta}$ the shear stress tangentially directed and acting on each circular fluid element of radius r. At the wall there is $v_r = 0$, which, put in formula (D) of [3] provides

$$\tau_{r,\theta} = -\mu r \frac{\partial}{\partial r} \left(\frac{v_\theta(r, t)}{r} \right). \tag{25}$$

Notice that by inserting the (17) in (25), the wall shear stress, as expected, can be determined only by the transient component of the velocity $\hat{v}(r, t)$. Fixing a particular time, we get the law of the shear stress in the fluid at different r values. Repeating the process for different times, we will describe the shear stress field with respect to time. When evaluating the stress for $t \to 0$, as physics suggests, $\tau_{r,\theta} = 0$. This can be explained in two different ways. The first consists of noting that for $t \to 0$ one shall have $\hat{v}(r, t) = \Omega r$ (initial condition previously set) and then, inserting it in (25) it is found $\tau_{r,\theta} = 0$. The second one consists of computing derivatives of $\hat{v}(r, t)$, and inserting in (25). A plot of the relevant curve for small times will show oscillations. But they are without any possible physical meaning and only due to the number of the terms chosen in order to represent $\hat{v}(r, t)$. As a matter of fact the number of terms which fits correctly a function, will not, in general, be used to do the same with its derivative. Accordingly, several computations and plots, here not attached, have been performed by making use of an adequate number of terms of the series for $\hat{v}$, and we checked that as their number increases, the pseudo-oscillation decay until to zero. After a threshold value $\bar{t}$, shear stress becomes as it follows.

Because of the onset of a transient circumferential component of velocity, this produces a darting to the shear stress for any r having its maximum at the wall. The

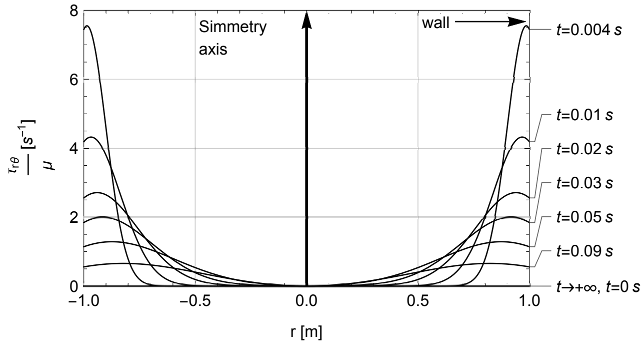

Figure 7. The shear stress $\tau_{r,\theta}$ unsteady response: radial profiles.

family of the stress profiles shown in Fig. 7 is decreasing quickly to equilibrium. After the circumferential stress has been computed as a function of r and time and it is specialised to $r = R$ and then by multiplying by $2\pi R$, we get the magnitude of the circumferential shear stress for unit height of the vessel.

5. Conclusions

The Navier-Stokes analytical unsteady equations have been investigated for the last 200 years and we outlined some of the most recent literature dealing with it. We study the unsteady viscous flow of an incompressible, isothermal (Newtonian) fluid whose motion is induced by the sudden swirling of a cylindrical wall and is also starting with an axial velocity component. In order to obtain an analytically tractable PDE system, our basic assumptions are (see our Subsection 1.3). Pressure axial gradient kept on its hydrostatic value and no radial velocity. By means of special functions and infinite series, we found the analytic solutions listed below.

The fluid motion has been decoupled in its simultaneous components separately studied, so that

- The *axial motion* differential equation (3) has been solved under the conditions (4), so that the relevant solution is found (7), plotted at Fig. 1.
- The *tangential motion* differential equation (11) has been solved under conditions (12), so that the relevant overall solution has been obtained (17) and plotted at Fig. 3.

  Furthermore

- The *pressure field* has been computed according to (20).

- The *liquid free surface* is found through (21), according to Subsection 3.4 and Fig. 5.

- Finally, Fig. 7 summarizes all the analyses concerning the *shear stress* unsteady response, discussed in detail at Subsection 4.2.

Appendix: Nomenclature

The main symbols recurring through this paper are:

- $C,\ D$ integration constants
- $\boldsymbol{k},\ \boldsymbol{e}_r,\ \boldsymbol{e}_\theta$ unity vectors axial, radial, tangential of the cylindric coordinate system
- g gravity acceleration
- $\boldsymbol{i},\ \boldsymbol{j},\ \boldsymbol{k}$ unity vectors of the Cartesian coordinate system
- $J_0,\ J_1,\ J_2$ Bessel functions of first kind and orders 0, 1, 2
- $P(r, z, t)$ pressure scalar field
- Q volume flow rate through the cylinder
- $r,\ \theta,\ z$ radial, angular, axial cylindrical coordinates
- R internal radius of cylindric wall
- t time
- $v_r,\ v_\theta,\ v_z$ radial, tangential, axial components of the $\boldsymbol{v}$ velocity field
- $v_\theta^\infty(r)$ steady tangential velocity component
- $\hat{v}(r, t)$ unsteady tangential velocity component
- Y_0 Bessel function of second kind and order 0
- $x,\ y,\ z$ Cartesian coordinates of a point
- $z(r, t)$ transient liquid free surface
- α_n sequence of zeros of J_1
- β_n sequence of zeros of J_0
- η, λ separation constants
- $\lambda_n = \frac{\alpha_n}{R}\sqrt{\nu}$ ease variable
- μ fluid dynamic viscosity
- ν fluid kinematic viscosity
- ρ fluid density
- $\sigma_n = \frac{\beta_n}{R}$, $b_n = \frac{\alpha_n}{R}$ ease variables
- $\tau_{r,\theta}$ tangential shear stress on fluid at r

• $\boldsymbol{\omega}$ angular speed vector

• Ω magnitude of angular speed

Some other few symbols have been used throughout the text as ease variables without a specific meaning and do not need to be listed here.

Acknowledgments

The last author is supported by an RFO grant issued by the Italian Ministry of University and research.

References

[1] Abramowitz M. and Stegun I., *Handbook of Mathematical Functions*: *With Formulas, Graphs, and Mathematical Tables*, Dover, New York 1972.

[2] Batchelor G., *An Introduction to Fluid Dynamics*, Cambridge Univ. Press, Cambridge 2000.

[3] Bird B., Stewart W. and Lightfoot E., *Transport Phenomena*, Wiley, New York 2002.

[4] Brenn G., *Analytical Solutions for Transport Processes*, Springer, Berlin 2017.

[5] Byrd R. B. and Curtiss C., *Tangential Newtonian Flow in Annuli-I. Unsteady State Velocity Profiles*, Chem. Eng. Sci. **11** (1959) 108–113.

[6] Drazin P. and Riley N., *The Navier-Stokes Equations*: *A Classification of Flows and Exact Solutions*, Cambridge Univ. Press, Cambridge 2006.

[7] Euler L., *Principes généraux du Mouvement des Fluides*, Mém. Acad. des Sci. Berlin **11** (1757) 274–315.

[8] Gatteschi L., *Funzioni Speciali*, UTET, Torino 1973.

[9] Gradshteyn I. and Ryzhik I., *Table of Integrals, Series, and Products*. Academic Press, New York 2007.

[10] Hayat T., Khan M. and Ayub M., *Some Analytical Solutions for Second Grade Fluid Flows for Cylindrical Geometries*, Math Comp. Mod. **43** (2006) 16–29.

[11] Knyazev D., *Axisymmetric Flows of an Incompressible Fluid Between Movable Rotating Disks*, Fluid Dyn. **46** (2011) 558–564.

[12] Lagerstrom P., *Laminar Flow Theory*, Princeton Univ. Press, Princeton 1996.

[13] Langlois W. and Deville M., *Slow Viscous Flow,* 2^{nd} Edn, Springer, Berlin 2014.

[14] McMahon J., *On the Roots of the Bessel and Certain Related Functions*, Ann. Math. **9** (1894) 23–30.

[15] Müller W., *Zum Problem der Anlaufströmung einer Flüssigkeit im geraden Rohr mit Kreisring-und Kreisquerschnitt*, Z. Angew. Math. Mech. **16** (1936) 227–238.

[16] Navier C. L., *Mémoire sur les Lois du Mouvement des Fluides*, Mém. Acad. Royale Sci. Inst. Fr. **6** (1823) 389–440.

[17] Polyanin A. and Zaitsev V., *Handbook of Exact Solutions for Ordinary Differential Equations,* 2^{nd} Edn, Chapman and Hall, London 2003.

[18] Shapiro A., *An Analytical Solution of the Navier-Stokes Equations for Unsteady Backward Stagnation-Point Flow with Injection or Suction*, Z. Angew. Math. Mech. **86** (2006) 281–290.

[19] Stokes G., *On the Theory of the Internal Friction of Fluids in Motion, and of the Equilibrium and Motion of Elastic Solids*, Trans. Cambridge Phil. Soc. **8** (1849) 287–319.

[20] Szymanski P., *Quelques Solutions Exactes des Équations d'Hydrodynamique du Fluide Visqueux dans le Cas d'un Tube Cylindrique*, J. Math. Pures Appl. **11** (1932) 67–108.

Alessio Bocci
Politecnico di Milano
20136 Milan, ITALY
E-mail address: alessio.bocci@live.it

Giovanni Mingari Scarpello
via Negroli 6
20133 Milano, ITALY
E-mail address: giovannimingari@yahoo.it

Daniele Ritelli
Department of Statistics
Bologna University
40126 Bologna, ITALY
E-mail address: daniele.ritelli@unibo.it